

Removing Heavy Metals from Industrial Wastewater Using Cement Kiln Dust and Electric Arc Furnace Dust as Industrial By-Products

S. A. Abo-El-Enein^{1*}, M. S. Attia¹, M. M. Ali², G. G. Mohamed³, M. S. S. Soliman²

¹Chemistry Department, Faculty of Science, Ain Shams University, Cairo, Egypt

²Chemistry Department, Central Laboratory for Environmental Quality Monitoring, National Water Research Center, Cairo, Egypt

³Chemistry Department, Faculty of Science, Cairo University, Cairo, Egypt

Corresponding author: saaboelenein@yahoo.com (S. A. Abo-El-Enein)

Tel: +202 01005363830

Abstract

The River Nile and its branches are the main source of fresh water in Egypt. They are subjected to all pollution sources, among and most important of it is the industrial one. This study aims to investigate removal efficiency of industrial wastewater discharged to Ismailia Canal using cement kiln Dust (CKD) and electric arc furnace dust (EAFD) as industrial adsorbents. Some heavy metals such as; iron, manganese, aluminum, nickel, and zinc have been studied. The adsorption process is examined in terms of its equilibria and kinetics. Batch adsorption experiments are performed to evaluate the removal of these metals onto CKD and EAFD by-product wastes under various operational conditions such as; adsorbate ions concentration, contact time, pH, adsorbent dose, and temperature. The results revealed that CKD has a very high affinity to adsorb iron, manganese, nickel, and zinc ions. While, EAFD can efficiently adsorb only manganese, aluminum and nickel. The adsorption isotherms and kinetic studies indicated that the adsorptive behavior of heavy metals ions on CKD and EAFD satisfy the Langmuir assumptions, i.e. monolayer formation on the surface of the adsorbent, and obeys the pseudo-second-order equation reaction.

Keywords

Heavy Metals Treatment, Cement Kiln Dust, Electric Arc Furnace Dust, Ismailia Canal, Adsorption and Langmuir Isotherm.

1. Introduction

Heavy metals, which are discharged to the surface water, is a global issue. They are difficult to degrade, but accumulate throughout the food chain, producing potential human health risks and ecological disturbances, biomagnification and accumulation in food chain. They are released into the environment through natural process and anthropogenic activities. The industrial processes generate wastes, which are mostly discharged into the water system. Industrial activities, especially electroplating, metal smelting and chemical industries, and manufacturing processes are few sources of anthropogenic heavy metals in water. Its presence in water is mainly due to industrial discharges, residential dwellings, and groundwater infiltration. The common heavy metals that have been identified in polluted water include arsenic, copper, cadmium, lead, chromium, nickel, iron, manganese, mercury and zinc. Severe effects include reduced growth and development, cancer, organ damage, and nervous system damage could happen due to their existence in the water system [1, 2]. The Egyptian industry uses about 7.8 Bm³/y of water, 65% of which comes from the River Nile system. There are 4.05 Bm³/y wastewater are discharged, as effluents, from these industries, 57% of which goes again to the Nile system [3, 4]. The risk of the heavy metal pollutants in water lies in two aspects. Firstly, the heavy metals have the ability to persist in natural ecosystems for an extended period. Secondly, they have the ability to accumulate in successive levels of the biological chain, thereby causing acute and chronic diseases. For example, cadmium and zinc can lead to acute gastrointestinal and respiratory damages [2]. Current treatment available technologies have major drawbacks; including high capital and operational costs, generation of toxic sludge, complicated operation and maintenance, and high energy consumption. Therefore, it is very essential to find an economically feasible, simple to operate, efficient and sustainable treatment method in order to protect our surface water bodies, eventually our health from heavy metals contamination. Conventional treatment system could not completely remove the heavy metals in the water, thus alternative purification methods using inexpensive materials were needed to improve the current treatment process. Wide ranges of low cost adsorbents were used to remove heavy metals in aqueous solution and wastewater. The low cost adsorbents such as; cement kiln Dust (CKD) and electric arc furnace dust (EAFD) as industrial adsorbents were usually collected from industrial by-products [5]. The main objective of the current research is to investigate the utilization of low cost waste materials as a sustainable solution

such as; (CKD) and (EAFD) for heavy metals such as; iron, manganese, aluminum, nickel, and zinc removal from industrial wastewater. The current research also aims to study the optimum operating conditions and the possible methods of application for the most successful material in the removal of heavy metals from industrial wastewater.

2. Methodology

2.1. Preparation of metal ions and analyses

Synthetic stock solutions of heavy metals are prepared by dissolving the required quantity of a metal salt in distilled deionized water. The salts used are $\text{FeSO}_4 \cdot 7\text{H}_2\text{O}$, $\text{MnCl}_2 \cdot 4\text{H}_2\text{O}$, anhydrous AlCl_3 , $\text{NiCl}_2 \cdot 6\text{H}_2\text{O}$ and $\text{Zn}(\text{NO}_3)_2 \cdot 6\text{H}_2\text{O}$. All preparations are performed at room temperature ($25 \pm 1^\circ\text{C}$) and at a constant stirring rate of 125 rpm. The concentrations of heavy metals are measured using the Inductively Coupled Plasma-Optical Emission Spectrometry (ICP-OES), Perkin Elmer Optima 5300, USA with Ultra Sonic Nebulizer (USN). Reagent grad concentrated hydrochloric acid and sodium hydroxide are used to adjust pH values of samples. The pH values are determined by bench-top pH/ISE meters.

2.2. Adsorbent Analyses

Cement Kiln Dust (CKD) used in this study is collected from the by-path of the National Cement Company, Cairo, Egypt. The received CKD is stored in a sealed glass container and it is used as received.

Electric Arc Furnace Dust (EAFD) is received from the Iron and Steel Co., Ataka, Suez, and it also is used as received.

Chemical analysis of adsorbents is determined by X-ray fluorescence (XRF) spectroscopy using an Axios, sequential WD- XRF spectrometer, PAN analytical 2005. The X-Ray powder diffraction (XRD) is analyzed using a PAN analytical X-ray Diffraction equipment model X Pert PRO. Adsorbent samples are investigated using scanning electron microscope (SEM) by Energy Dispersive X-Ray Analysis Spectrometry EDAX ZAF qualification standardless sec. kV:20.00 Tilt:0.00 Take-off:32.97 AmpT:102.4 Detector Type:SUTW-Sapphire Resolution :129.66. While the surface area is measured using a Quantachrome NovaWin instrument (version 11.03) with nitrogen gas as the analysis gas.

2.3. Batch adsorption study

The removal of heavy metal ions by each of CKD and EAFD is carried out using the batch method. Batch adsorption experiments are conducted using 0.1 g of adsorbent to 100 mL of solution containing heavy metal ions of determined concentrations (depending on the adsorbent affinity to each element) of Fe²⁺, Mn²⁺, Al³⁺, Ni²⁺ and Zn²⁺ ions at constant temperature (25±1°C). The experiments are performed by shaking the weighed solid sorbent with the metal ion solution in a 250 ml conical flask in a shaker at a 125 rpm rate. After the required time, the conical flask is removed and the adsorbent is isolated by filtration through a 45µm Whatman filter paper. The filtrate is analyzed by ICP-OES. The percent of heavy metal removal efficiency is calculated using equation (1):

$$\% \text{ Removal Efficiency} = \frac{(C_0 - C_e)}{C_0} \times 100 \quad (1)$$

where, C₀ is the initial concentration of metal ion (mg L⁻¹)

C_e is the metal ion concentration after adsorption (mg L⁻¹)

The removal efficiency is investigated under various conditions such as pH, contact time, initial metal concentration, and solution temperature. The following part illustrates these variables:

2.4.1. Effect of initial metal ion concentration

The effect of initial metal ion concentration on the removal percent is examined at fixed adsorbent dose (0.1 g) and different metal ion concentrations (from 5 to 500 mg/L) to 100 mL of solution for 180 minutes.

2.4.2. Adsorption kinetic study (contact time)

In these preliminary studies, the contact time necessary to reach equilibrium was investigated. Different flasks are treated following the procedure above and the samples are taken at predetermined time intervals ranging from 5 to 180 min. From this experiment, the required time for the maximum removal (equilibrium time) is defined as the time after which is considered a wasted time.

2.4.3. Effect of pH

After identifying the working concentration and time for each element, different pH values have been investigated from 1 to 8, using HCl and NaOH for adjusting the pH values.

2.4.4. Effect of temperature

The temperature effects on the adsorption capacity of the two adsorbents are investigated for the metal ions. Three different temperature values of 35, 45 and 55 °C are chosen at fixed concentration, time, and pH.

2.4.5. Effect of adsorbent dose and time

Different doses of adsorbent (0.05, 0.1, 0.15, 0.2, 0.25 and 0.3 g) have been added to 100 mL of solution at different time from 5 minutes to the determined one at the identified constant concentration, time, and pH.

2.4.6. Effect of Stirring rate

Different stirring rates (100, 200, 300, 400 and 500 rpm) have been investigated.

2.4.7. Isotherm Modeling

Adsorption equilibrium is defined as the equilibrium distribution of a given component between an adsorbate and adsorbent. Langmuir, Freundlich and Temkin isotherm equations are examined to describe the equilibrium adsorption. The equations of isotherms are given below:

2.4.7.1. Langmuir isotherm

The Langmuir isotherm derived from simple mass action kinetics is based on the assumptions that molecules are adsorbed as a saturated monolayer of one molecule thickness with no transmigration in the plane of the surface, and interaction between adsorbed molecules are negligible with energy of adsorption remaining constant. The linear form of the Langmuir isotherm model can be presented as [6]:

$$\frac{C_e}{q_e} = \frac{C_e}{Q_0} + \frac{1}{Q_0 K_L} \quad (2)$$

where q_e (mg/g) is the amount of the phenol adsorbed per unit mass of adsorbent, C_e (mg/L) is the equilibrium phenol concentration in the solution, Q_0 (mg/g) is the Langmuir constant related to the maximum monolayer adsorption capacity, and K_L (Lmg^{-1}) is the constant related to the free energy or net enthalpy of adsorption. The linear plot of C_e/q_e versus C_e indicates that adsorption obeys the Langmuir model, and the constants Q_0 and K_L are obtained from the slope and intercept of the linear plot, respectively.

The essential features of the Langmuir isotherm model can be expressed in terms of ' R_L ' a dimensionless constant, separation factor or equilibrium parameter, which is defined by the following equation:

$$R_L = \frac{1}{1 + K_L C_0} \quad (3)$$

where C_0 (mg L^{-1}) is the initial amount of adsorbate and K_L (Lmg^{-1}) is the Langmuir constant described above. The R_L parameter is considered as more reliable indicator of the adsorption. There are four probabilities for the R_L value:

- for favorable adsorption $0 < R_L < 1$,
- for unfavorable adsorption $R_L > 1$,
- for linear adsorption $R_L = 1$ and
- for irreversible adsorption $R_L = 0$.

2.4.7.2. *Freundlich isotherm*

The Freundlich isotherm is an empirical equation used for non-ideal adsorption on heterogeneous surfaces as well as multilayer adsorption and is derived by assuming an exponentially decaying adsorption site energy distribution, which can be expressed as [7]:

$$q_e = K_F C_e^{1/n} \quad (4)$$

Where, K_F ($\text{L}^n \text{mg}^{1-n}/\text{g}$) is the Freundlich constant related to the adsorption capacity and n is the Freundlich exponent (dimensionless). The Freundlich model in linear form:

$$\ln q_e = \ln K_F + \frac{1}{n} \ln C_e \quad (5)$$

where K_F (mg g^{-1}) is the constant related to the adsorption capacity and n is the empirical parameter related to the intensity of adsorption. The value of n varies with the heterogeneity of the adsorbent and for favorable adsorption process the value of n should be less than 10 and higher than unity. The values of K_F and $1/n$ are determined from the intercept and slope of linear plot of $\ln q_e$ versus $\ln C_e$, respectively.

3. Results & Discussion

3.1. Adsorbent identification

Identification of CKD and EAFD adsorbents

Chemical analysis of CKD and EAFD samples by X-ray fluorescence (XRF) spectroscopy is presented in table (1 and 2). While, the mineralogical characteristics of them are illustrated in tables (3 and 4). The main constituting phases of CKD are calcium oxide (CaO) and quartz (SiO_2) and the main ones of EAFD are iron and zinc. The measured surface areas of them equal to 3.288 and 1.019 m^2/gm respectively.

Table 1 : The oxide composition of CKD under investigation.

Chemical Analysis											
SiO ₂	Al ₂ O ₃	Fe ₂ O ₃	CaO	MgO	SO ₃	Na ₂ O	K ₂ O	Cl	Total	H ₂ O	CaCO ₃
14.52	4.03	2.81	46.93	1.98	4.27	5.97	3.16	8.60	92.27	0.00	0.00
14.44	3.98	3.04	58.26	2.42	3.94	2.14	1.23	2.80	92.35	0.00	0.00
14.48	4.01	2.93	52.60	2.20	4.11	4.06	2.20	5.71	92.26	0.00	0.00

Table 2 : The chemical composition of EAFD.

Element	Wt%	Element	Wt%
Al	0.22	Cr	0.53
Mg	1.49	Mn	2.67
Si	0.35	Zn	36.33
Cl	3.78	Cu	0.19
K	3.51	Pb	1.74
Ca	3.59	Sn	0.17
Fe	35.77	Others	0.29
		Total	90.63

Table 3: Energy dispersive X-ray spectroscopy of CKD.

Element	Wt%	At %
<i>CK</i>	25.23	44.11
<i>OK</i>	20.18	26.49
<i>MgK</i>	00.51	00.44
<i>AlK</i>	00.56	00.44
<i>SiK</i>	01.43	01.07
<i>SK</i>	00.70	00.46
<i>ClK</i>	00.98	00.58
<i>CaK</i>	50.39	26.40

Table 4: Energy dispersive X-ray spectroscopy of EAFD.

Element	Wt %	At %
<i>CK</i>	12.19	25.20
<i>OK</i>	24.46	37.96
<i>MgK</i>	01.86	01.90
<i>AlK</i>	03.21	02.96
<i>SiK</i>	03.88	03.43
<i>CaK</i>	24.95	15.46
<i>MnK</i>	02.74	01.24
<i>FeK</i>	26.71	11.87

3.2. Batch Study

CKD and EAFD are used to remove selected metal ions (Fe²⁺, Mn²⁺, Al³⁺, Ni²⁺ and Zn²⁺) from wastewater. Therefore many parameters had been studied: effect of concentration, effect of time, effect of pH, effect of stirring, effect of adsorbent dose, and effect of temperature. The alkalinity nature of both types of dust adsorbents made

them good neutralizing agents even for acidic wastewater stream, but not for the very acidic one, where at pH equals 2 or less the very acidic medium analyzes the adsorbent and even released more ions to the solute. In general, both types of dust increase the pH value of the solution to the alkaline medium. The chemical analysis of CKD showed that sodium and potassium oxides had dominant effect on the increase of the pH of the aqueous CKD [8] and similarly the potassium occurrence in EAFD composition that forms the oxide compound in the aqueous medium, raises the pH too. The mechanism of heavy metals removal from acidic wastewater may be explained as follows:

1. Heavy metals hydrolysis:



Where X : Na or K

M : Fe, Mn, Al, Ni, or Zn

Y : SO_4^{2-} , Cl^- , or NO_3^- depending on the salt used

n : 2 or 3

2. Adsorption of heavy metals on adsorbent:



Where $Ads.$: CKD or EAFD

3.2.1. Effect of initial metal ion concentration

Tables (5 and 6) show the concentrations at which each adsorbent gave the higher removal percentage. From table (5), it can be seen that the CKD adsorbent had no steady state toward the aluminum metal, and in some times the adsorbent lose some atoms and increase the Al concentration than the initial one. This can be attributed to the big Al-atom and its low density (about one third as much as the iron atom) that gave it the unstable state [9]. This also can be attributed to that the adsorbent itself contained Al compound (Al_2O_3) as a main component. So, the Al metal had been excluded from the rest of the study. Also table (6) shows that EAFD could not adsorb Fe and Zn ions from their solutions, and this is attributed to the chemical composition of the EAFD adsorbent that shows that Fe and Zn are the main components of the adsorbent and the adsorbent itself releases some iron and zinc ions to the solution.

Figure (1) illustrates the relation between the initial concentration in mg/L and the removal percentage to the metals by CKD, and in general the removal is increased gradually with concentration till a specific concentration (that differ from metal to other) after which the removal percentage decreases. While, figure (2) shows the corresponding relations for Mn, Al, and Ni ions by EAFD.

Table 5 : Effect of initial concentration by CKD.

Metal	Concentration (mg/L)	Removal %
Fe	8	91
Mn	80	99.42
Al	---	---
Ni	250	99.11
Zn	200	100

Table 6: Effect of initial concentration by EAFD.

Metal	Concentration (mg/L)	Removal %
Fe	---	---
Mn	10	98.85
Al	20	100
Ni	20	99.92
Zn	---	---

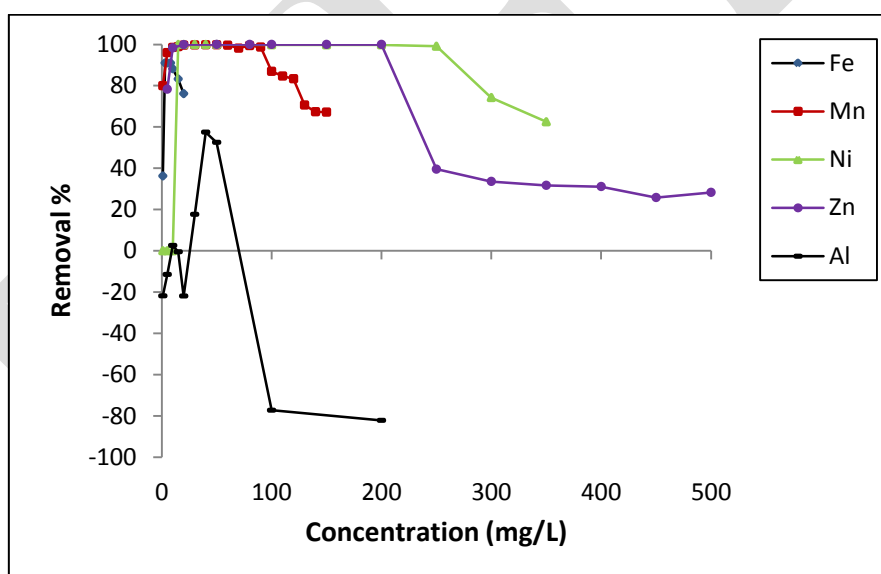


Figure 1: Initial metal ions concentrations versus removal (%) using CKD as an adsorbent.

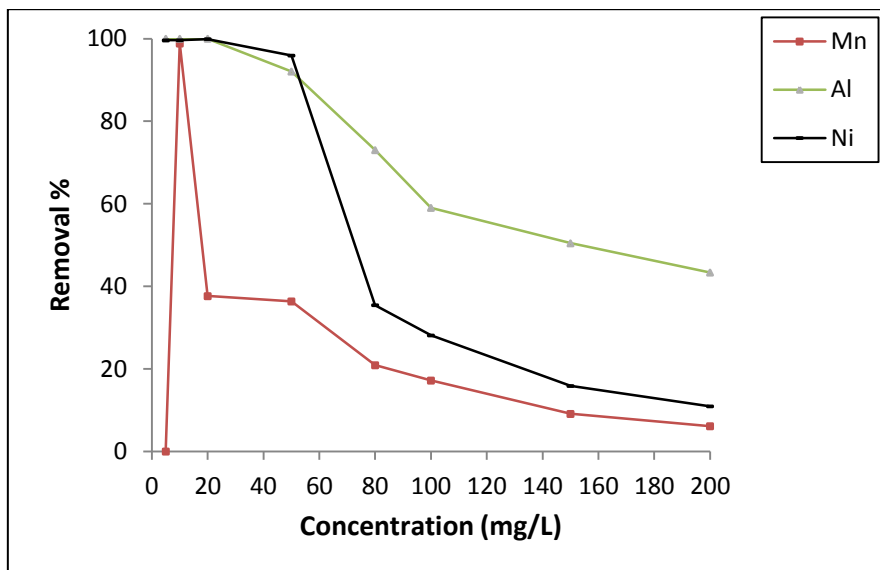


Figure 2: Initial metal ions concentrations versus removal (%) using EAFD as an adsorbent.

3.2.2. Effect of contact time

After identifying the initial concentration to each element, the equilibrium time at which the adsorption process stops (the adsorbent is separated by filtration using a 0.45µm whattman filter paper), must be determined where after that time the adsorbent would not remove any more metal. It is considered losing time if the reaction continued. From figure (3), it is concluded that the equilibrium times are 60, 30, 90, and 120 minutes for Fe, Mn, Ni, and Zn, respectively for CKD adsorption reactions. While, the equilibrium times of Mn, Al, and Ni by EAFD are 60, 5, and 30 minutes respectively (figure 4).

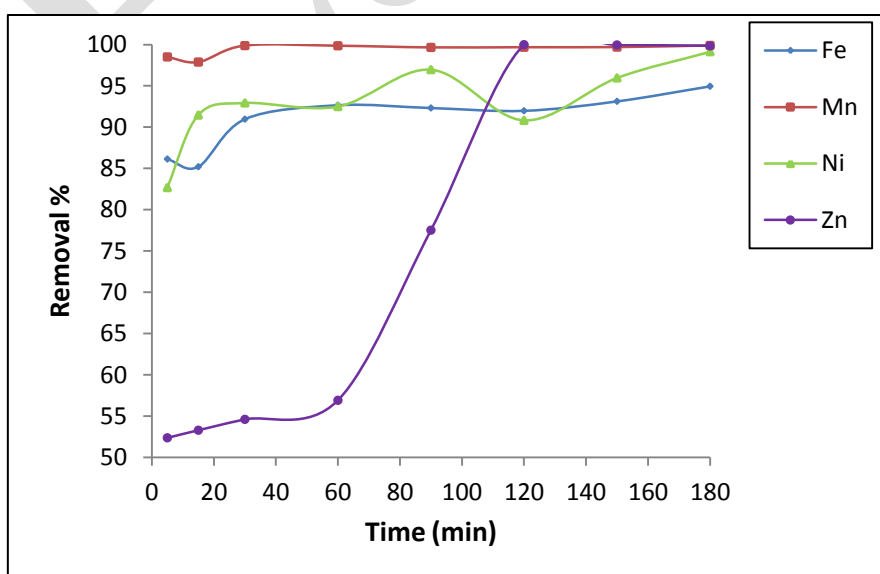


Figure 3: Contact time versus removal (%) using CKD as an adsorbent.

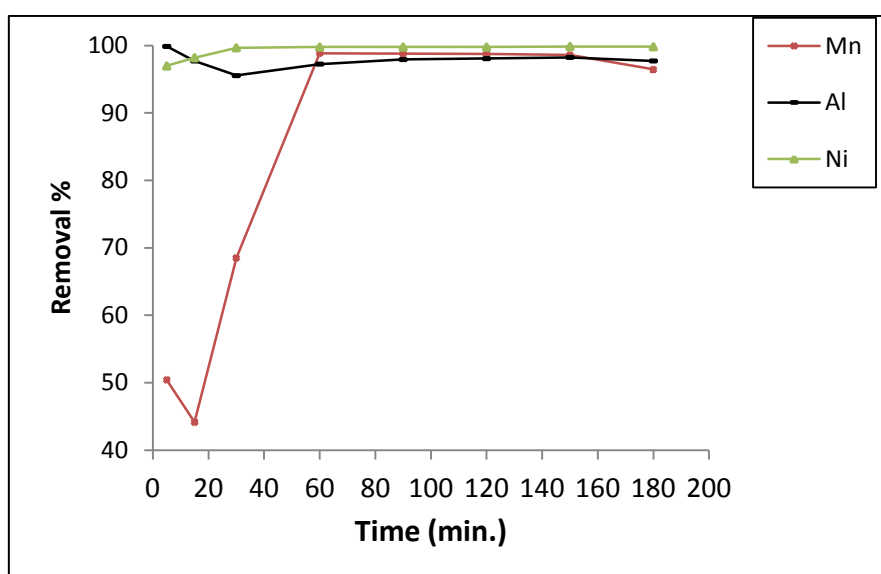


Figure 4: Contact time versus removal (%) using EAFD as an adsorbent.

3.2.3. Effect of pH

CKD adsorbent dissociates at pH equals 1, while EAFD at $\text{pH} \leq 2$. The metals under investigation precipitate at different pH values. According to **Balintova, M. and A. Petrilakova (2011) [10]** manganese ions precipitate at pH range equals 6:8, aluminum ions at 4:5.5 and zinc ions at 5:8. While iron ions precipitate at 4:8 [11] and nickel ions at $\text{pH} \geq 7$ [12]. With taking this information into consideration, the effect of pH by both adsorbents was studied for each metal at pH less than the dissociation pH (figures 5 and 6). It was found that the removal percentage of the prepared solutions for all metal ions without changing the pH had almost no significant difference with the one at the optimum pH. The difference had not exceeded 2%, so for all metals the other effects have been done without changing their pH.

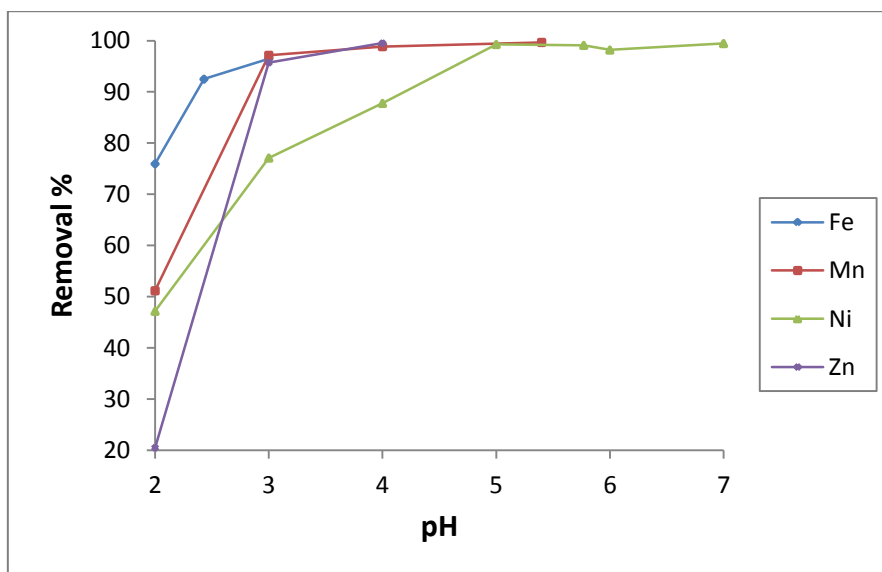


Figure 5: pH versus removal (%) using CKD as an adsorbent.

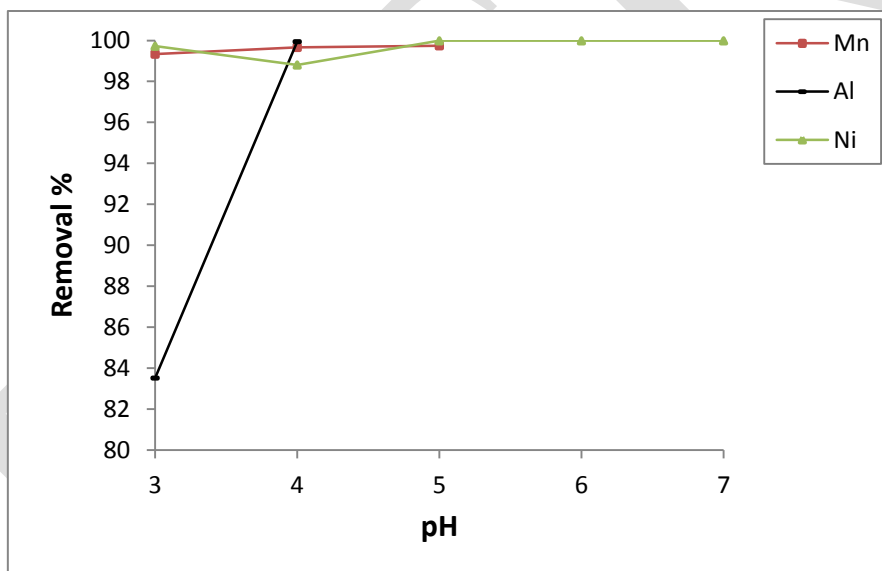


Figure 6: pH versus removal (%) using EAFD as an adsorbent.

3.2.4. Effect of stirring

In general the removal percentage had a slight increase with increasing the stirring rate (from 100 to 500 rpm). Figures (7, 8) illustrate this behavior.

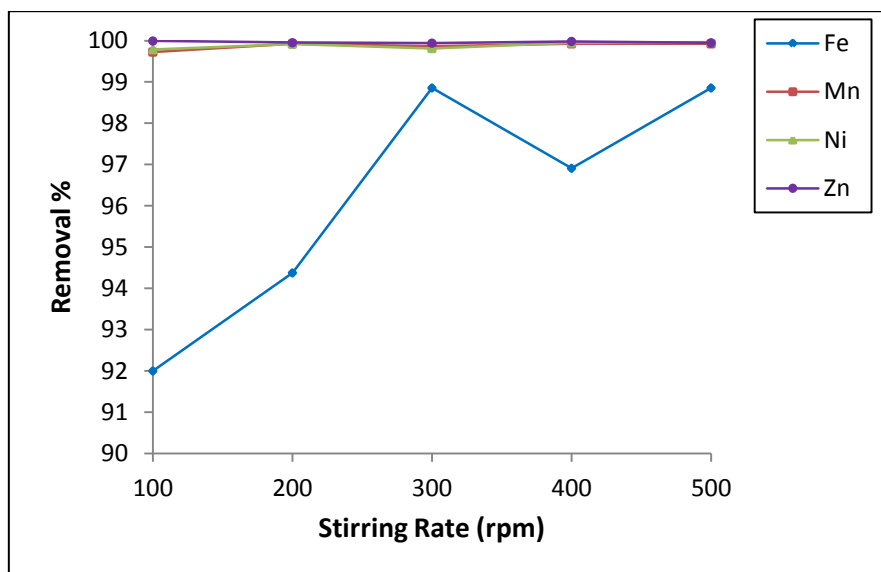


Figure 7: Stirring rate versus removal (%) using CKD as an adsorbent.

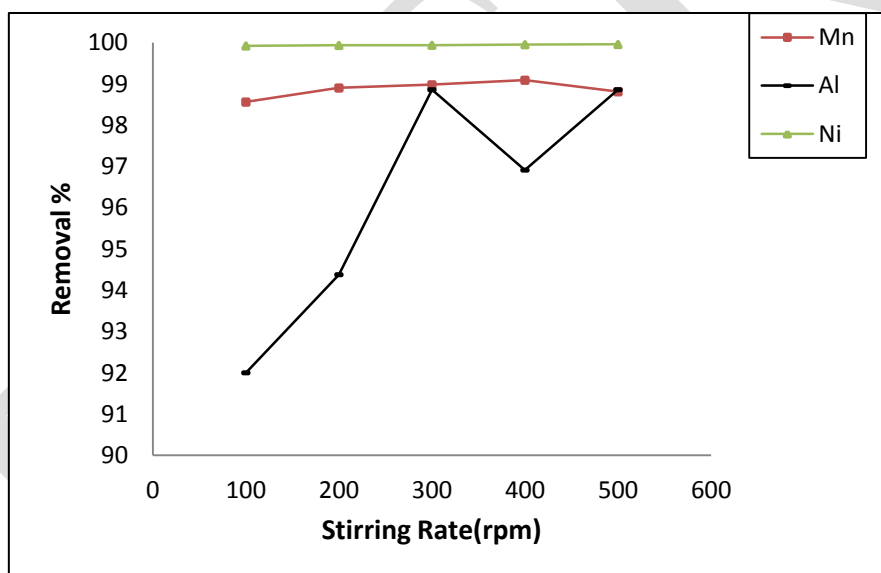


Figure 8: Stirring rate versus removal (%) using EAFD as an adsorbent.

3.2.5. Effect of adsorbent dose with time

Different adsorbent doses, from 0.05 to 0.3 g, had been added to 100 mL of the metal solutions for different time intervals from 5 min to the equilibrium time of each metal, i.e. to 60, 30, 90, and 120 min for Fe, Mn, Ni, and Zn, respectively for CKD, and to 60, 5, and 30 min for Mn, Al, and Ni respectively for EAFD. Figures (9-15) illustrate this effect. In all cases as the dose increased, the removal percentage increased too. Also as the time increased, the removal % increased.

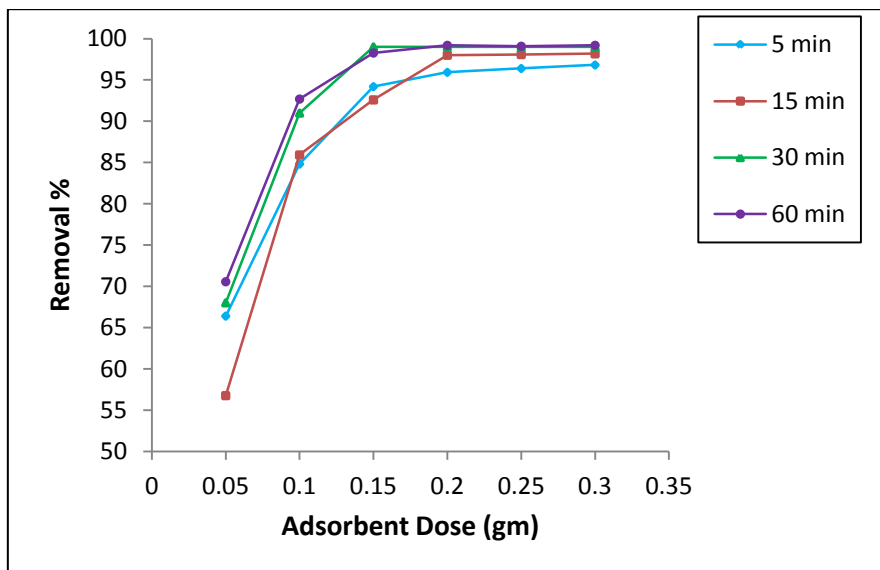


Figure 9: Adsorbent dose versus removal (%) at different time intervals for the removal of Fe(II) using CKD as adsorbent.

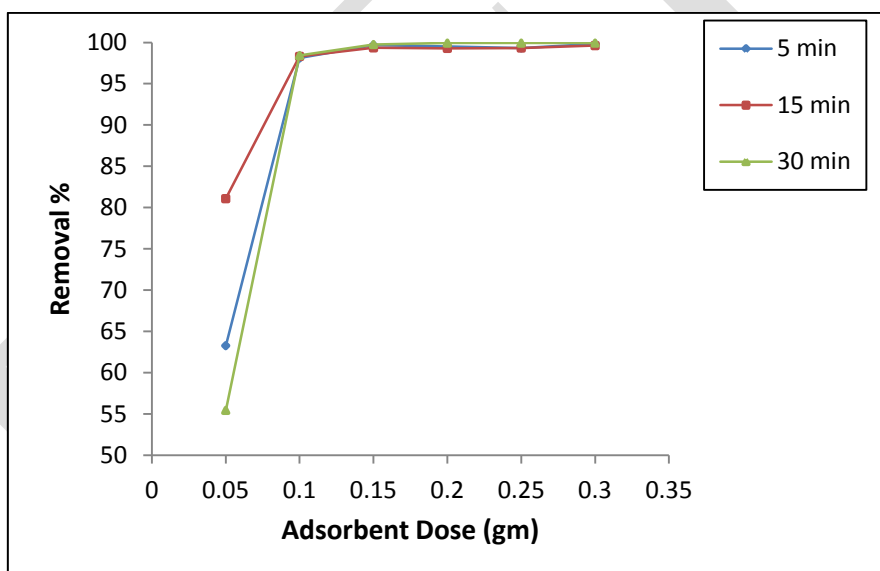


Figure 10: Adsorbent dose versus removal (%) at different time intervals for the removal of Mn(II) using CKD as adsorbent.

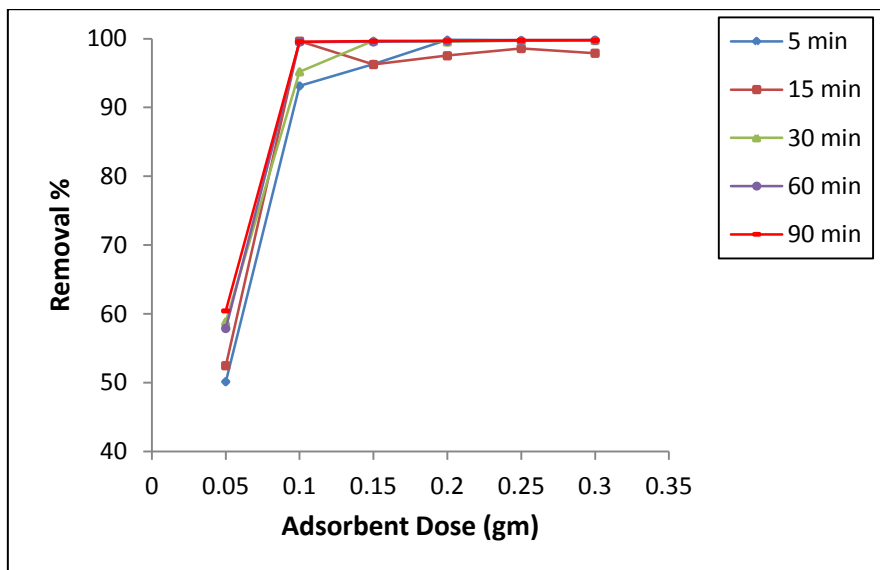


Figure 11: Adsorbent dose versus removal (%) at different time intervals for the removal of Ni(II) using CKD as adsorbent.

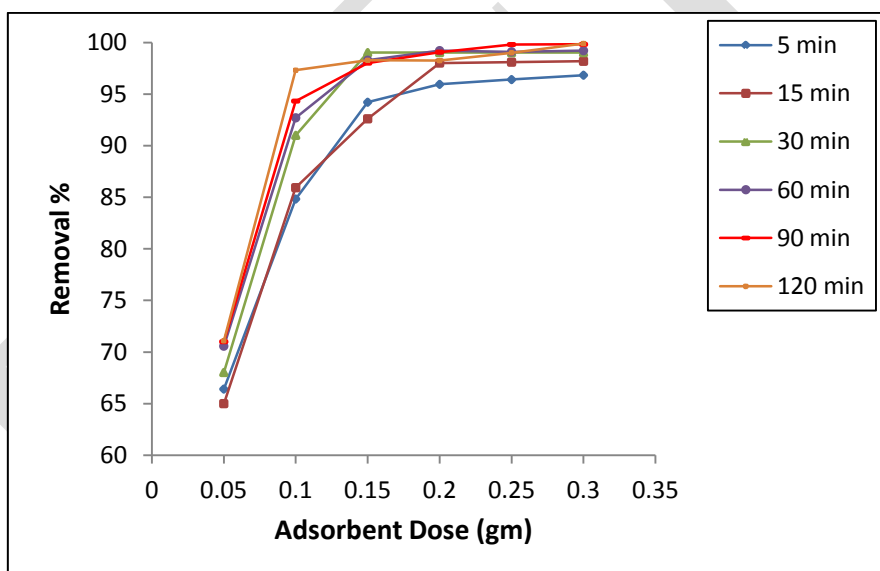


Figure 12: Adsorbent dose versus removal (%) at different time intervals for the removal of Zn(II) using CKD as adsorbent.

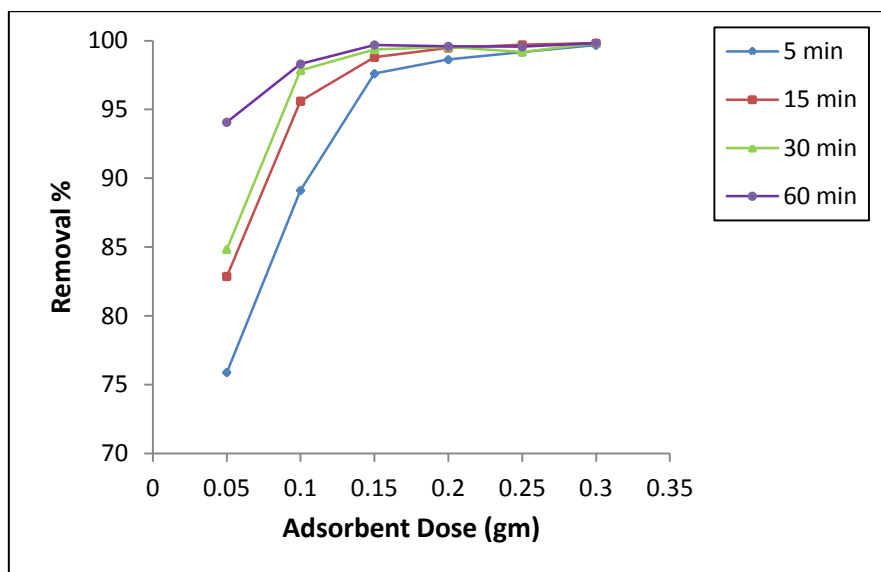


Figure 13: Adsorbent dose versus removal (%) at different time intervals for the removal of Mn(II) using EAFD as adsorbent.

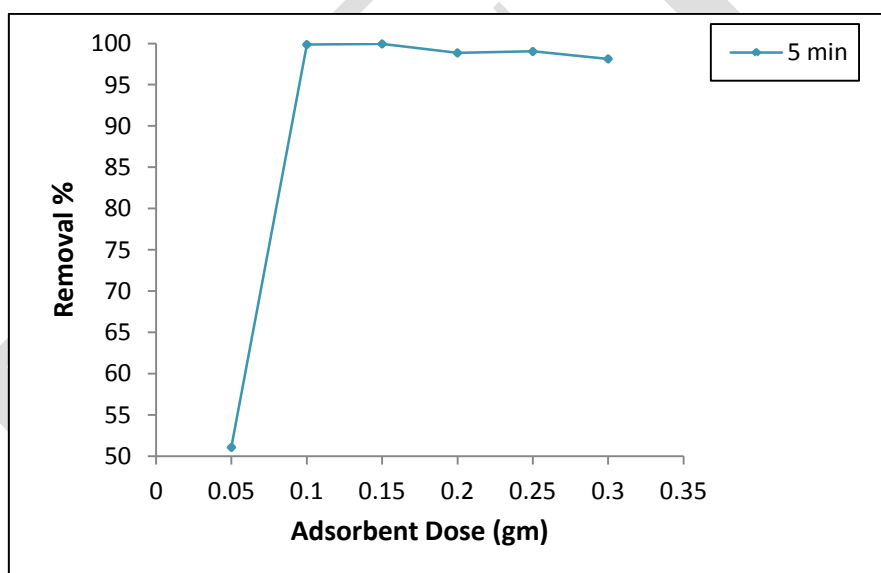


Figure 14: Adsorbent dose versus removal (%) at different time intervals for the removal of Al(III) using EAFD as adsorbent.

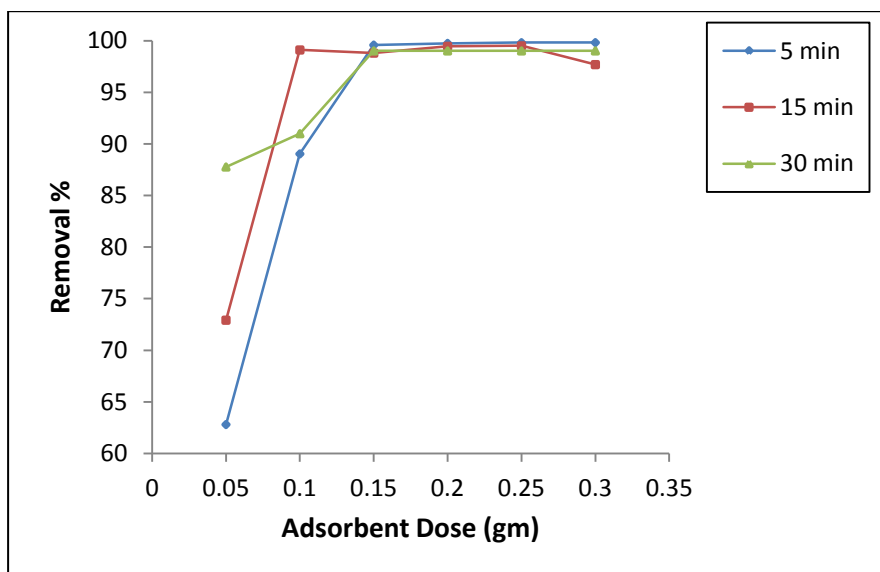


Figure 15: Adsorbent dose versus removal (%) at different time intervals for the removal of Ni(II) using EAFD as adsorbent.

3.2.6. Effect of temperature

The removal efficiency has been studied at 25, 35, 45, and 55 °C. For CKD adsorbent: Fe and Mn had almost no change with increasing the temperature, while Ni and Zn removal percentage decreased with increasing the temperature. While in the case of EAFD, the temperature has almost no effect for all metals (figures 16, 17).

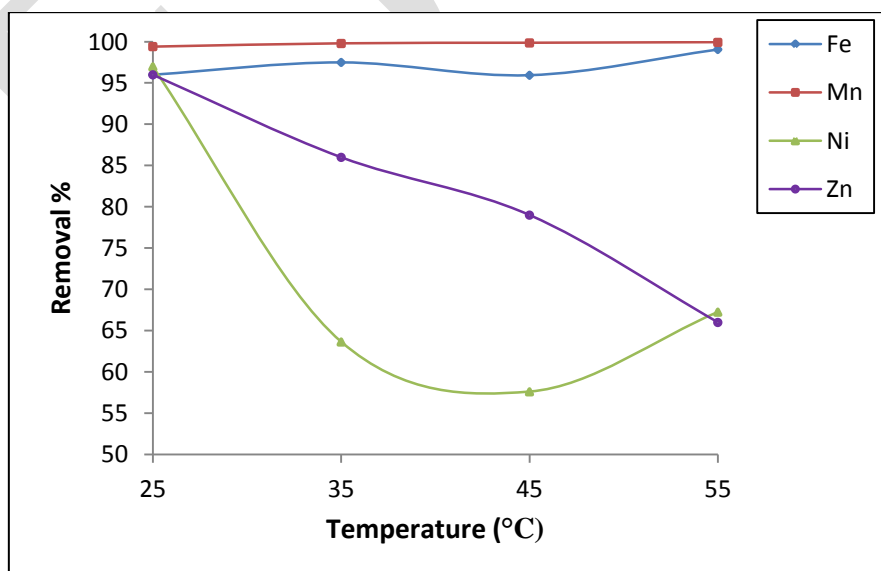


Figure 16: Temperature versus removal (%) using CKD as an adsorbent.

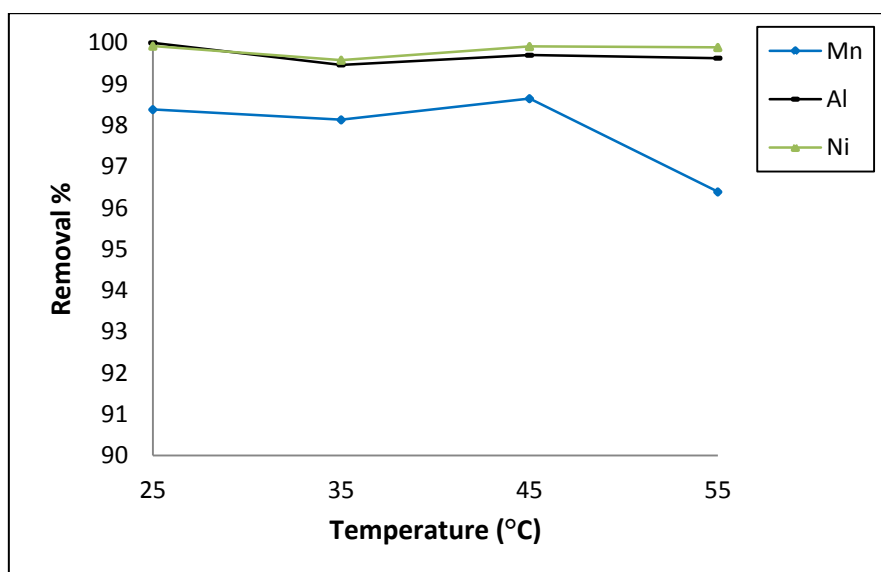


Figure 17: Temperature versus removal (%) using EAFD as an adsorbent.

3.3. Adsorption Isotherm and Thermodynamics

The adsorption studies are conducted at fixed initial concentration of heavy metals. The equilibrium data obtained are analyzed in the light of Langmuir isotherm (equation 2), and Freundlich isotherm (equation 5). Figure (18) shows the relation between C_e/q_e and C_e for applying Langmuir equation to each metal by CKD, and Figure (19) presents the relation between $\ln(q_e)$ and $\ln(C_e)$ for the Freundlich isotherm. And figures (20, 21) represents the corresponding applications by EAFD. Tables (7, 8) display the intercepts, slopes and constants that are extracted from the two equations by CKD, respectively, and tables (9, 10) show it but by EAFD adsorbent.

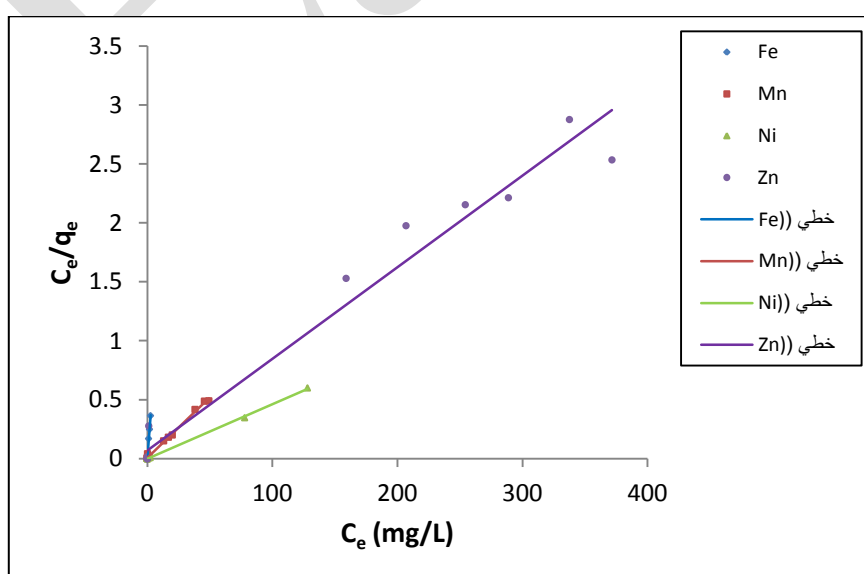


Figure 18: C_e/q_e versus C_e for Langmuir isotherm application using CKD as adsorbent.

Table 7: Constants of Langmuir isotherm for the adsorption of heavy metals using CKD.

Metal	R ²	Slope	Intercept	Q _{max}	K _L	R _L
Fe	0.9922	0.1398	0.0104	7.15	13.44	0.0084
Mn	0.995	0.0103	0.0077	97.09	1.34	0.0093
Ni	0.9993	0.0046	0.0006	217.39	7.67	0.0005
Zn	0.9744	0.0078	0.0715	128.21	0.109	0.0448

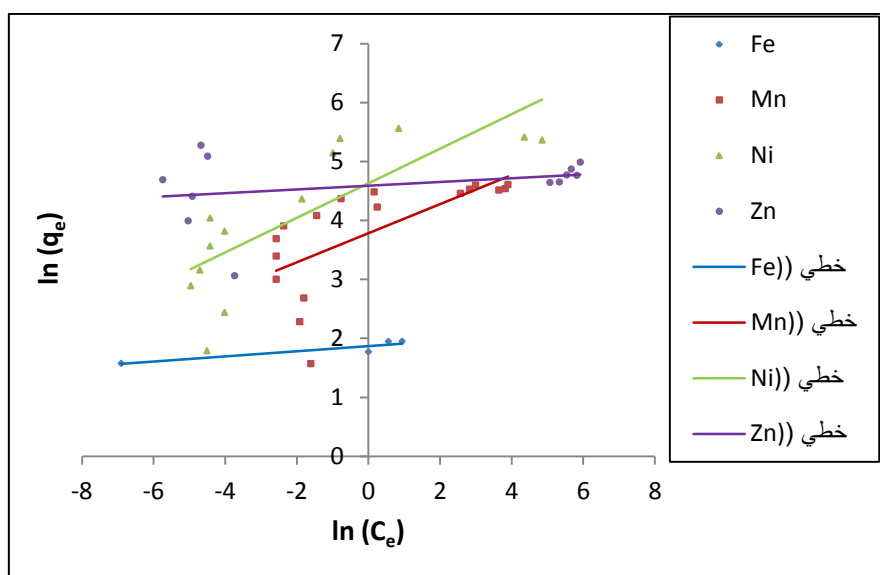


Figure 19: $\ln(q_e)$ versus $\ln(C_e)$ for Freundlich isotherm application using CKD as adsorbent.

Table 8: Constants of Freundlich isotherm for the adsorption of heavy metals using CKD.

Metal	R ²	Slope	Intercept	n	K _f
Fe	0.8518	0.044	1.871	22.73	6.49
Mn	0.4629	0.2469	3.7844	4.05	44.01
Ni	0.6327	0.2936	4.6298	3.41	102.49
Zn	0.0843	0.0313	4.5888	31.95	98.38

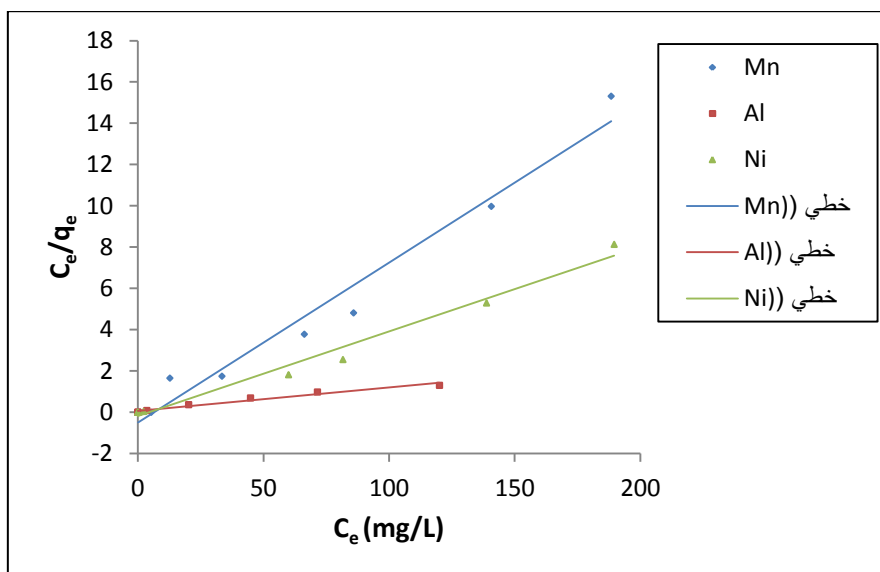


Figure 20: C_e/q_e versus C_e for Langmuir isotherm application using EAFD as adsorbent.

Table 9: Constants of Langmuir isotherm for the adsorption of heavy metals using EAFD.

Metal	R^2	Slope	Intercept	Q_{max}	K_L	R_L
Mn	0.9709	0.0775	-0.5009	12.903	-0.1547	-1.522
Al	0.9677	0.0114	0.0583	87.72	0.1955	0.207
Ni	0.9838	0.041	-0.1891	24.39	-0.217	-0.264

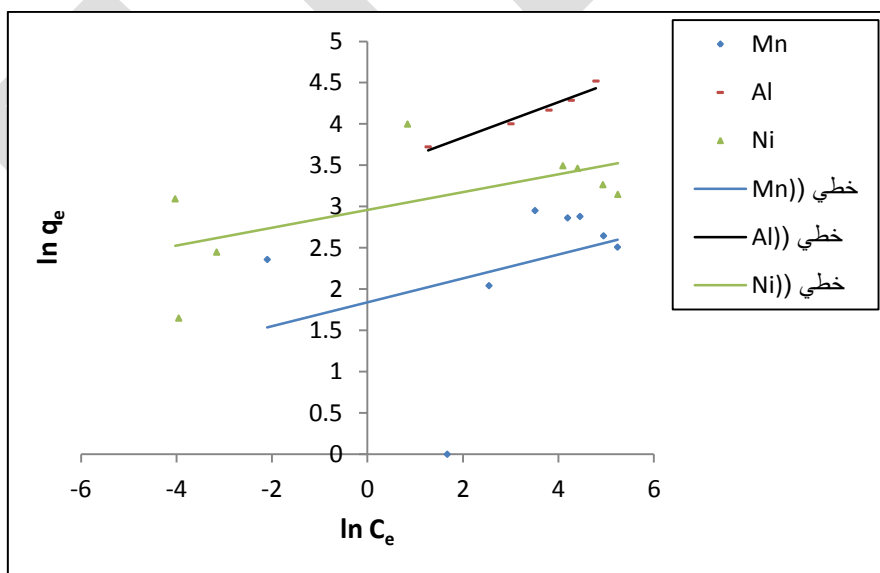


Figure 21: $\ln(q_e)$ versus $\ln(C_e)$ for Freundlich isotherm application using EAFD as adsorbent.

Table 10: Constants of Freundlich isotherm for the adsorption of heavy metals using EAFD.

Metal	R ²	Slope	Intercept	n	K _f
Mn	0.1287	0.1448	1.839	6.9	6.29
Al	0.9554	0.2137	3.4083	4.68	30.214
Ni	0.3865	0.1076	2.9582	9.294	19.263

The adsorption isotherm studies clearly indicate that the adsorptive behavior of heavy metal ions on both CKD and EAFD satisfy, with good agreement, the Langmuir assumptions, i.e. monolayer formation on the surface of the adsorbent. This can be attributed to three main causes (i) the formation of monolayer coverage on the surface of the adsorbents with minimal interaction among molecules of substrate (ii) immobile and localized adsorption and (iii) all the sites have equal adsorption energies. The shapes of isotherms suggested that there are high-energy adsorption sites to favor strong adsorption at low equilibrium concentrations for the CKD [13].

The kinetic parameters are determined from the linear plot of $\log (q_e - q_t)$ vs time (t) for pseudo-first-order (PFO) reaction as shown in figure (22) of CKD and figure (24) of EAFD, and of (t/q_t) vs t for pseudo-second-order (PSO) one as shown in figure (23) of CKD and figure (25) of EAFD. The validity of each model is checked by the fitness of the straight line (R^2) as well as the consistence between experimental and calculated values of q_e . The data was found to fit well (R^2 exceeded 0.95) the pseudo-second order model as shown in Tables (12 and 14). Meanwhile the data is found not to fit the pseudo-first order model as indicated from the value of calculated q_e compared to q_e obtained experimentally beside R^2 values (Tables 11 and 13). Adsorption may take place through a multi-step mechanism comprising; (i) external film diffusion, (ii) intraparticle diffusion and (iii) interaction between adsorbate and active site [14].

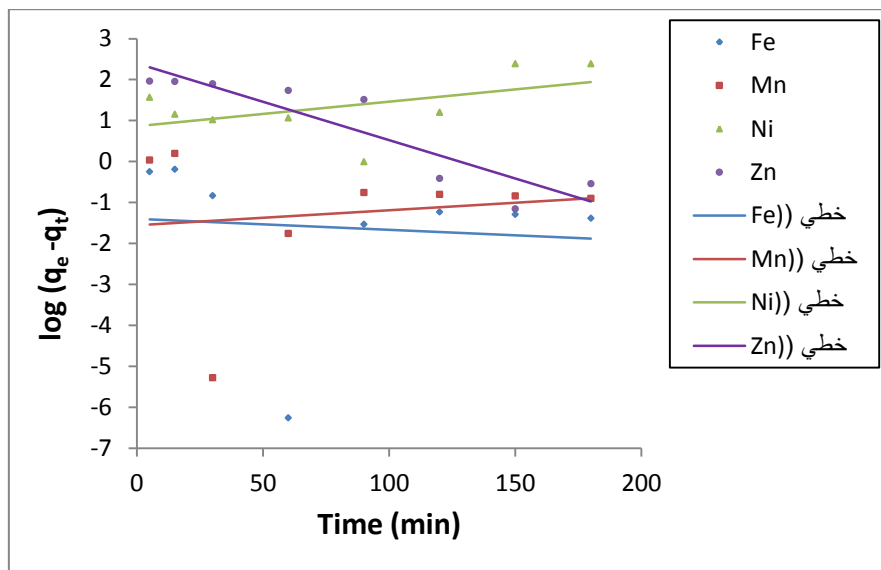


Figure 22: $\log (q_e - q_t)$ versus time for the PFO reaction using CKD adsorbent.

Table 11: Constants of PFO equation for the adsorption of heavy metals using CKD.

Metal	R ²	Slope	Intercept	K ₁	experimental q _e	calculated q _e
Mn	0.0082	-0.0027	-1.3964	0.0062	7.42	0.04
Al	0.0189	0.0037	-1.5565	-0.0085	79.34	0.0277
Ni	0.2448	0.006	0.8667	-0.0138	254.54	7.357

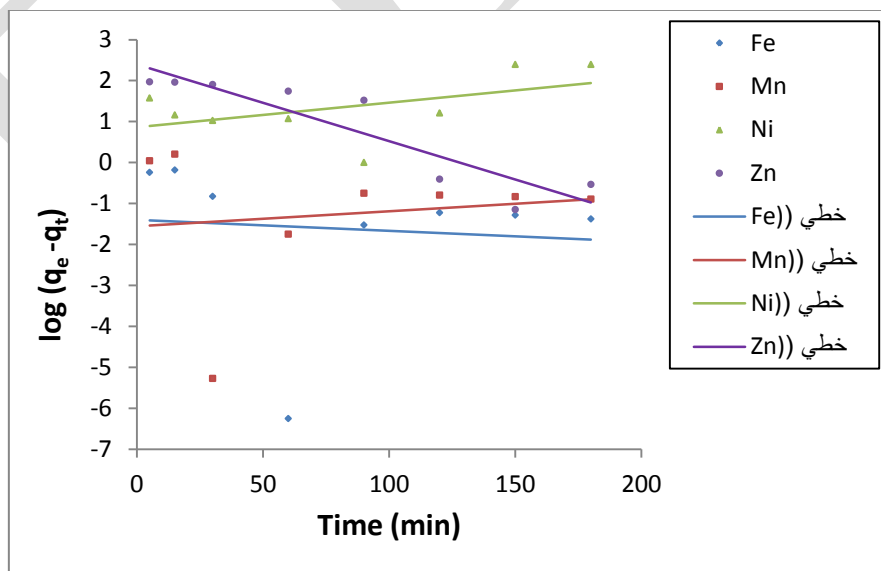


Figure 23: $\log (q_e - q_t)$ versus time for the PFO reaction using CKD adsorbent.

Table 12: Constants of PSO equation for the adsorption of heavy metals using CKD.

Metal	R ²	Slope	Intercept	K ₂	experimental q _e	calculated q _e
Fe	0.9996	0.1318	0.2102	0.174	7.42	7.40
Mn	1	0.0126	0.0012	0.0625	79.34	80
Ni	0.9973	0.0039	0.0082	0.0031	254.54	256.41
Zn	0.9575	0.0049	0.0786	0.0003	195.26	204.08

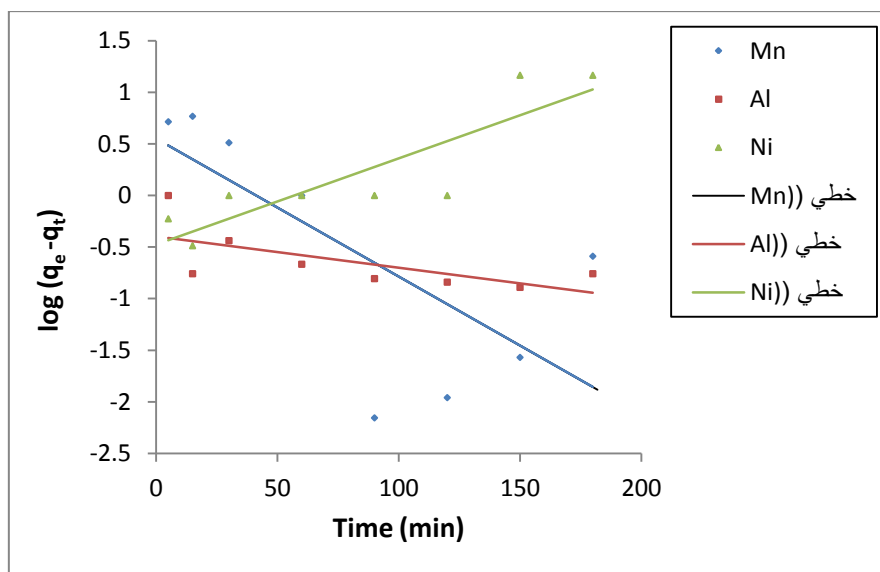


Figure 23: log (q_e-q_t) versus time for the PFO reaction using EAFD adsorbent.

Table 13: Constants of PFO equation for the adsorption of heavy metals using EAFD.

Metal	R ²	Slope	Intercept	K ₁	experimental q _e	calculated q _e
Mn	0.5062	-0.0134	0.5519	0.05757	10.587	0.9933
Al	0.4418	-0.003	-0.398	0.0069	19.5847	0
Ni	0.7621	0.0083	-0.4751	-0.019	22.0162	0.3349

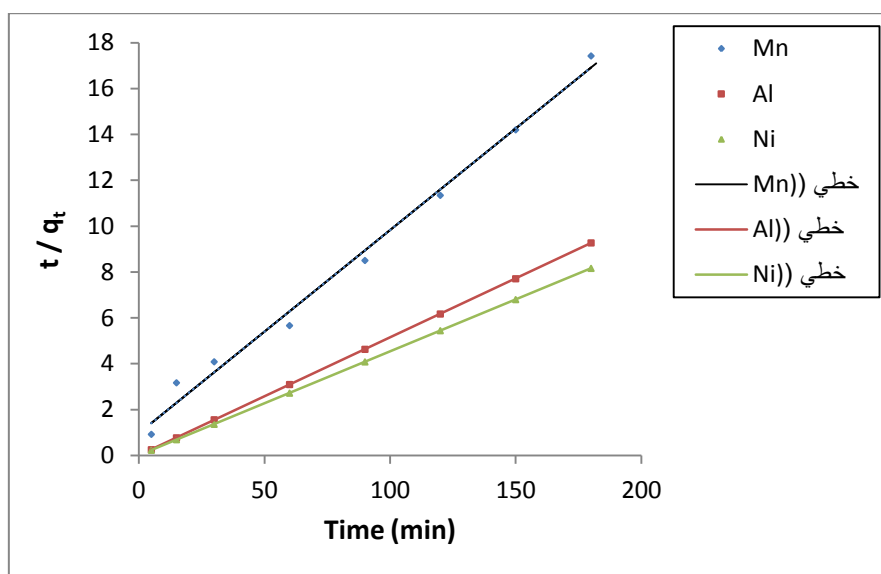


Figure 24: t/q_t versus time for the PSO reaction using EAFD adsorbent.

Table 14: Constants of PSO equation for the adsorption of heavy metals using EAFD.

Metal	R^2	Slope	Intercept	K_2	experimental q_e	calculated q_e
Fe	0.9909	0.0887	0.9642	0.00815	10.587	11.27
Mn	1	0.0514	0.0051	0.518	19.5847	19.455
Ni	1	0.0453	0.0068	0.3018	22.0162	22.075

Tables (15, 16) show the thermodynamic parameters for each element by the two adsorbents. From the Gipp's free energy values, it is clear that the adsorption of iron and manganese ions is spontaneous, while the adsorption reaction of nickel and zinc is a non-spontaneous one by CKD adsorbent. While, the adsorption process of manganese, aluminum, and nickel by EAFD is spontaneous.

Table 15: The chemical thermodynamic parameters of the ions adsorption by CKD.

Metal Ion	ΔH°	ΔS°	Temp. (K)	ΔG°
Iron	-104.25	7.52	298	-2344.72
			308	-2419.90
			318	-2495.08
			328	-2570.27
Manganese	754.55	72.72	298	-20915.53
			308	-21642.71

			318	-22369.90
			328	-23097.08
Nickel	-1128.29	-20.24	298	4903.85
			308	5106.27
			318	5308.69
			328	5511.11
Zinc	-747.80	-2.74	298	67.81
			308	95.18
			318	122.55
			328	149.92

Table 16: The chemical thermodynamic parameters of the ions adsorption by EAFD.

Metal Ion	ΔH°	ΔS°	Temp (K)	ΔG°
Manganese	-194.42	27.21	298	-8304
			308	-8576.14
			318	-8848.27
			328	-9120.40
Aluminum	-2228.48	95.25	298	-30614.03
			308	-31566.56
			318	-32519.1
			328	-33471.63
Nickel	-44.11	53.64	298	-16027.42
			308	-16563.77
			318	-17100.13
			328	-17636.48

4. Conclusion

In this study, batch adsorption experiments are conducted to evaluate the use of CKD and EAFD particles as adsorbents for five heavy metals (iron, manganese, aluminium, nickel, and zinc). It is found that manganese has required the shortest contact time 30 min, while equilibrium is reached for zinc after about 2 hrs for the adsorption by CKD. And for EAFD, the aluminum ions adsorption took only five minutes, and manganese took the longest time which is 60 minutes

It is found that there was no need to change the solutions pH, because the difference in removal percentage between it and the optimum one is slightly low. Most of the metal ions has a removal percentage that exceeded 90% except for Al ions by CKD and Fe, Zn ions by EAFD, as the adsorbent could not adsorb it because of its unstable state and also because the adsorbent itself contained them in its components.

The adsorption isotherm studies clearly indicated that the adsorptive behavior of the metal ions on CKD and EAFD satisfied the Langmuir assumptions, i.e. monolayer formation on the surface of the adsorbent, and obeyed to the pseudo-second-order reaction isotherm.

The results of this study have shown that CKD and EAFD cheap by-products of cement and steel industries respectively are effective in the removal of most of the ions in the study.

References:

- Chowdhury, S., M.J. Mazumder, O. Al-Attas, and T. Husain, *Heavy metals in drinking water: Occurrences, implications, and future needs in developing countries*. Science of The Total Environment, 2016. **569**: p. 476-488.
- Akpor, O. and M. Muchie, *Remediation of heavy metals in drinking water and wastewater treatment systems: Processes and applications*. International Journal of Physical Sciences, 2010. **5**(12): p. 1807-1817.
- Shamruk, M. and A. Abdel-Wahab, *Water Pollution and Riverbank Filtration for Water Supply Along River Nile, Egypt*, in Book *Riverbank Filtration for Water Security in Desert Countries*, M. Shamruk, Editor. 2011.
- Donia, N. and H. Farage, *Development of the Nile River Water Quality Information System*, in *First International Conference 2005*: Ain Shams University, Egypt.
- Lim, A.P. and A.Z. Aris, *A review on economically adsorbents on heavy metals removal in water and wastewater*. Reviews in Environmental Science and Bio/Technology, 2014. **13**(2): p. 163-181.
- Langmuir, I., *The adsorption of gases on plane surfaces of glass, mica and platinum*. Journal of the American Chemical society, 1918. **40**(9): p. 1361-1403.
- Freundlich, U., *Die adsorption in lusungen*. 1906.
- Hameed, B., A. Ahmad, and N. Aziz, *Adsorption of reactive dye on palm-oil industry waste: equilibrium, kinetic and thermodynamic studies*. Desalination, 2009. **247**(1): p. 551-560.
- Tahir, S. and N. Rauf, *Thermodynamic studies of Ni (II) adsorption onto bentonite from aqueous solution*. The Journal of Chemical Thermodynamics, 2003. **35**(12).

- Balintova, M. and A. Petrilakova, *Study of pH influence on selective precipitation of heavy metals from acid mine drainage*. Chem Eng Trans, 2011. **25**: p. 345-350.
- Morgan, B. and O. Lahav, *The effect of pH on the kinetics of spontaneous Fe (II) oxidation by O₂ in aqueous solution—basic principles and a simple heuristic description*. Chemosphere, 2007. **68**(11): p. 2080-2084.
- Janyasuthiwong, S., E.R. Rene, G. Esposito, and P.N. Lens, *Effect of pH on Cu, Ni and Zn removal by biogenic sulfide precipitation in an inversed fluidized bed bioreactor*. Hydrometallurgy, 2015. **158**: p. 94-100.
- Taha, A., A. Dakrouy, G. El-Sayed, and S. El-Salam, *Assessment removal of heavy metals ions from wastewater by cement kiln dust (CKD)*. Journal of American Science, 2010. **6**(12): p. 910-917.
- Yousif, S.S. *Removal of some pollutants from aqueous solutions using modified cellulose*. Master Thesis in Chemistry, 2013. Faculty of Science, Menoufia University.